Supplementary information

A facile strategy for the ion current and fluorescence dual-lock in detection: naphthalic anhydride azide (NAA)-modified biomimetic nanochannel sensor towards H_2S

I Wu, Dan Zhang,* Xuanjun Zhang*

Faculty of Health Sciences, University of Macau, Macau SAR 999078, China

*Emails: yb97663@um.edu.mo (D. Zhang); xuanjunzhang@um.edu.mo (X. Zhang)

Supporting Figures

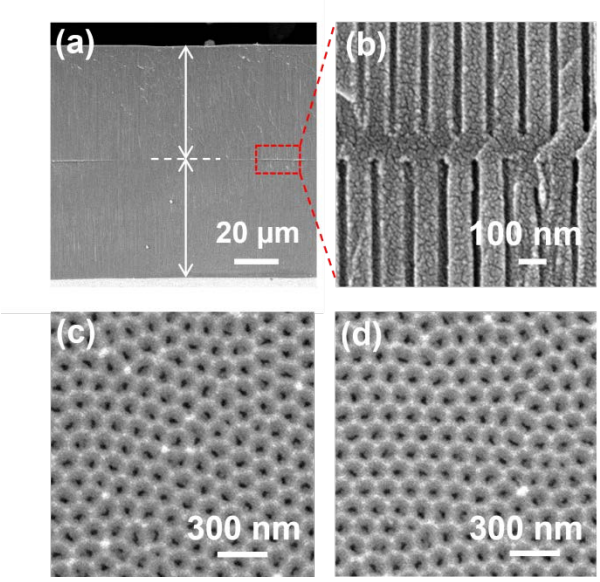

Figure S1: SEM images from the cross-section view at (a) low and (b) high magnification as well as its (c) top and (d) bottom surface view of the hourglass-shaped alumina nanochannel, respectively.

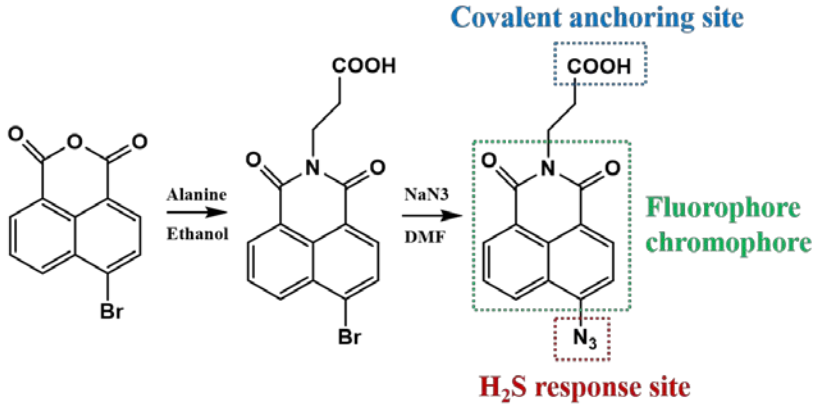

Figure S2: The synthesis of naphthalic anhydride-azide probe by the two-step substitution reaction at different positions of 4-bromo-1,8-naphthalic anhydride. The resulted probe fuses fluorescence chromophore (naphthalic anhydride), covalent anchoring site, and specific H_2S response site. Such structure configuration is convenient for covalently immobilizing the responsive element to the nanochannel without affecting its response characteristics.

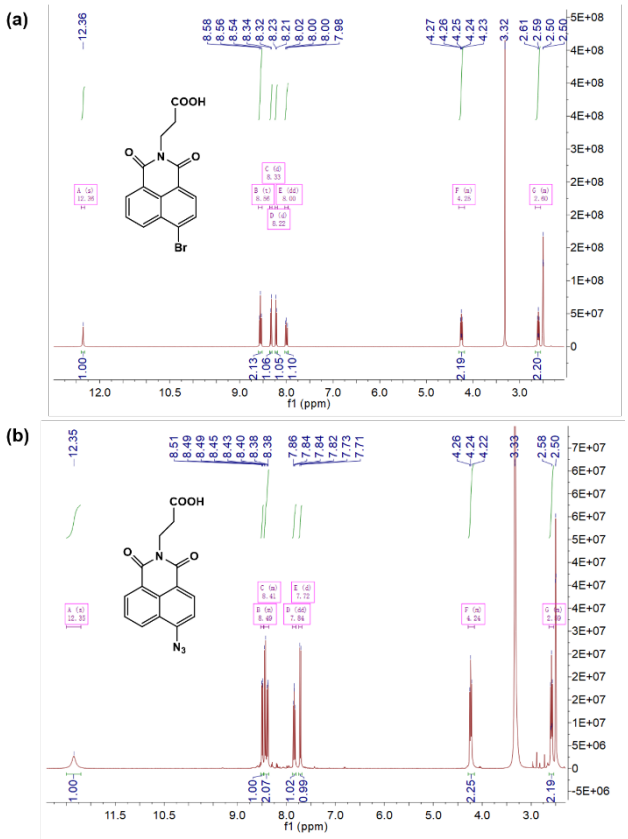

Figure S3: The ^{1}HNMR spectrum of (a) mediate compound and (b) naphthalic anhydride-azide probe molecules.

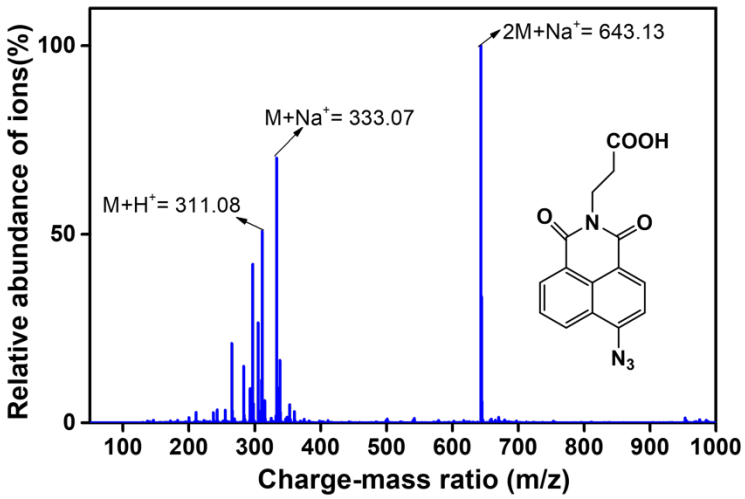

Figure S4: The MS of naphthalic anhydride-azide probe molecules.

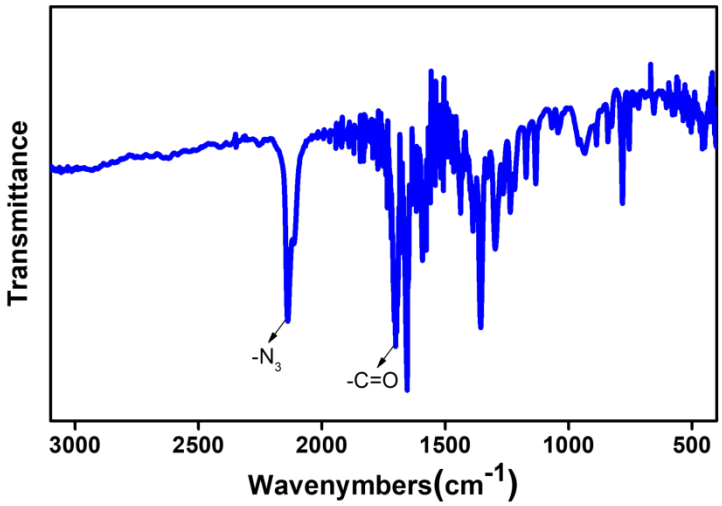

Figure S5: The IR spectrum of naphthalic anhydride-azide probe molecules. The characteristic stretching vibration peak of $-N_3$ at about 2130 cm^{-1} and of -C=O at about 1701 cm^{-1} can be observed. The results showed that the carboxyl group and azide group appeared on the anhydride structure after the reaction.

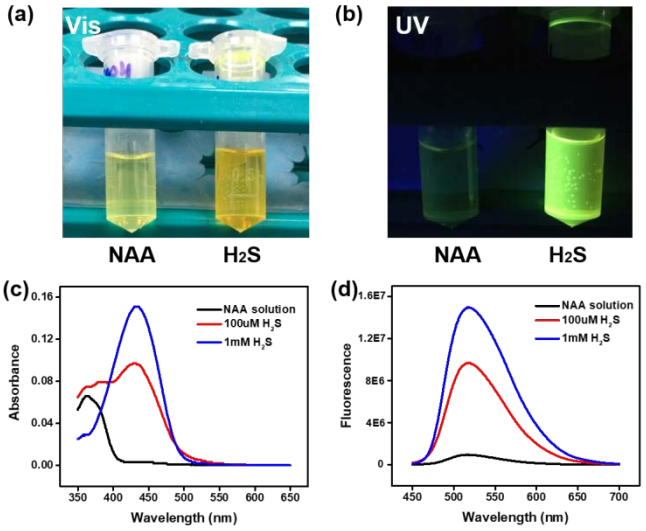

Figure S6: The photograph images of probe solution under (a) visible and (b) ultraviolet irradiation without and with H_2S. (c) UV-Vis absorption spectra and (d) fluorescence spectra of probe solution (10 μM) with the addition of 10 equiv. and 100 equiv. NaHS.

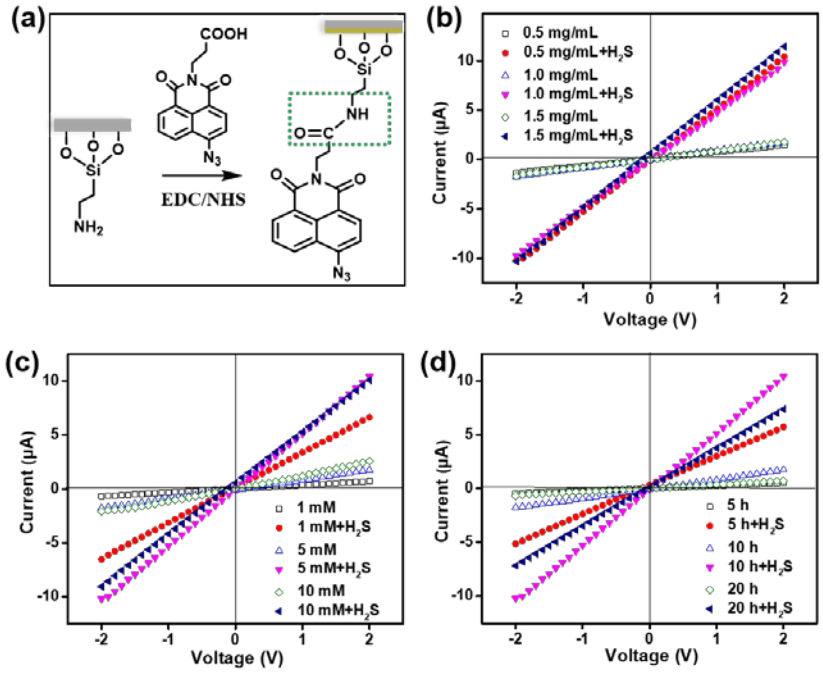

Figure S7: (a) A diagram of carboxylic-amino condensation between the probe and APTES-modified channel into amide using EDC/NHS coupling. *I-V* curves of NAA channel before and after H_2S stimulus with (b) different EDC/NHS concentration, (c) different probe solution, and (d) different modification time.

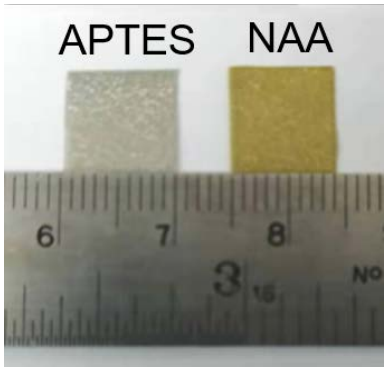

Figure S8: Optical photograph nanochannels before and after modification of probe molecules. The color of the membrane turned yellow from semi-transparent silver.

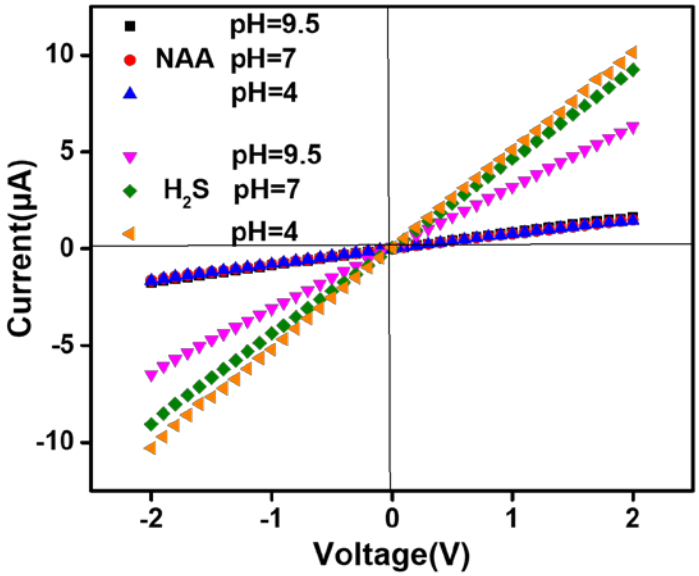

Figure S9: The pH-dependent *I-V* curve measurements of functionalized nanochannels before and after treatment with 1mM NaHS.

We have measured the *I-V* properties of the functionalized nanochannels before and after the treatment with NaHS using KCl electrolytes with pH values of 4.0, 7.0, and 9.5, respectively. As shown in Figure S9, for NAA nanochannels, no change in transmembrane ion current could be observed as the pH of the electrolyte changes. This is because the azide groups on the channel surface do not change with the pH of the electrolyte. Differently, after the treatment with 1mM NaHS, we found that the ionic current across the nanochannel membrane would increase to a certain extent with the decrease of pH. Compared with pH≈9.5, the ion current of the nanochannels in the pH≈7.0 environment increased due to the higher positive charge on inner walls caused by amino protonation. Further lowering the pH to 4, the ionic current across the membrane increased slightly. Perhaps because the amino protonation is approaching saturation in neutral environments. So further lowering the pH has little effect on the ion current change. The pH-dependent measurements indirectly demonstrated the successful conversion of azide groups to amino groups.

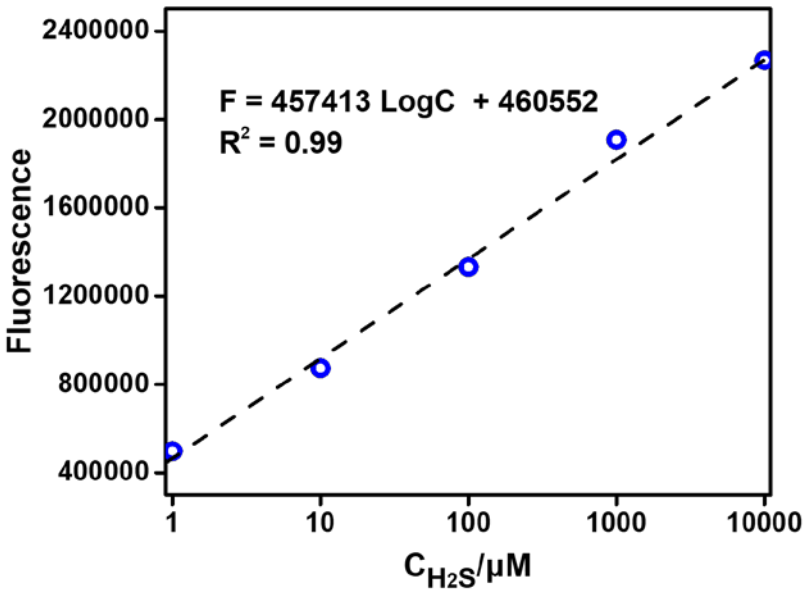

Figure S10: The quantitative linear relationship between the fluorescence (F) at 521 nm with the Logarithm (LogC) of H_2S concentration.

Quantification of fluorescence signal intensity with hydrogen sulfide concentration is important for practical applications. To show the regularity of fluorescence intensity upon H_2S treatment, the fluorescence (F) at 521 nm was employed as the quantitative signal. The F values versus the logarithm of H_2S concentrations (LogC) show a linear relationship over the range from 1 μM to 10 mM. As displayed in Figure S10, the linear regression equation can be represented as F = 457413 LogC + 460552 with a correlation coefficient of 0.99. According to 3 SD/N methods (SD is the standard deviation of the blank, N is the slope of the calibration curve), the lowest detection limit is calculated as 71.5 nM. Combined with the current signal, photoelectric quantification provides the possibility of more accurate detection of H_2S for the photoelectric dual response.

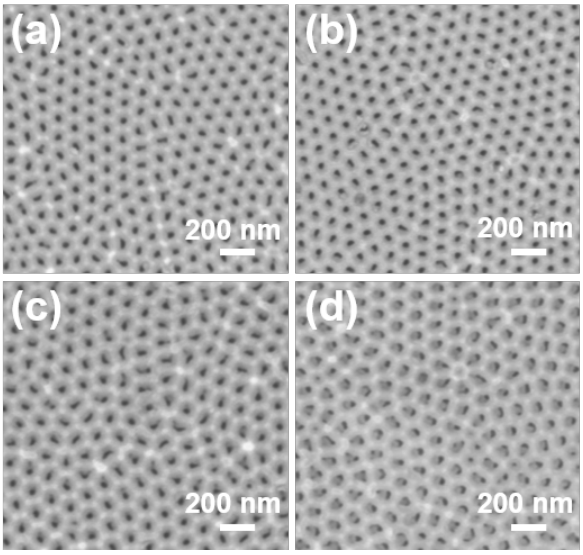

Figure S11: SEM images of the top surface of (a) alumina nanochannels, (b) APTES-modified nanochannels, (c) probe-modified nanochannels, and (d) nanochannels treated by 1 mM NaHS as H_2S source.

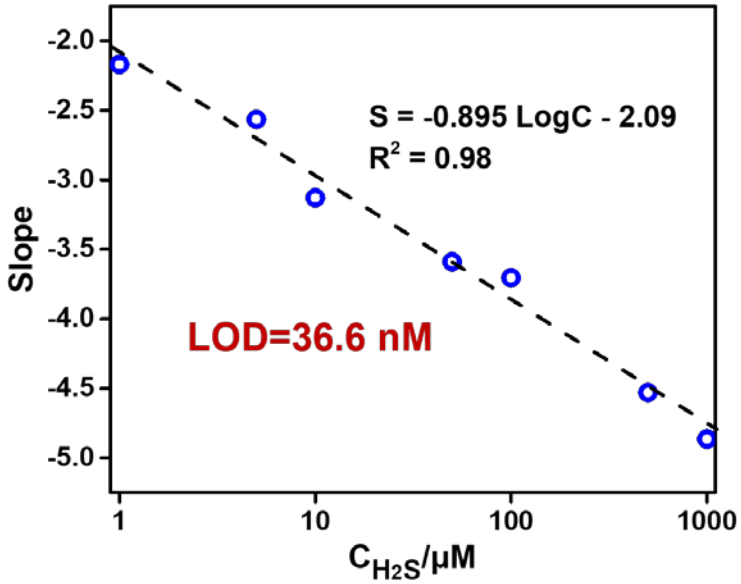

Figure S12: The linear relationship between the slope of *I-V* curves with the H_2S concentration. The lowest detection limit is estimated as 36.6 nM.

We have built an analytical curve by varying the slope (S) of the straight *I-V* curves as a function of the H_2S concentration (LogC), as plotted in Figure S12. The slope is calculated using an ion current at the – 2 V voltage divided by 2 (obtained by Figure 4c). The results show that in the range of hydrogen sulfide concentration from 1 uM to 1 mM, the linear calibration equation is described as S = -0.895 LogC - 2.09, with a correlation coefficient of 0.98. According to the 3 SD/N methods (SD represents the standard deviation of the blank sample, which is 0.01092 here; N represents the slope of the calibration curve, which is 0.895 here), the lowest detection limit of the H_2S sensor is estimated as 36.6 nM. This is in good agreement with the detection limit result obtained by the linear curve between current difference and hydrogen sulfide concentration (Figure 4d).